

Slide 1

QUANTIFYING THE LIKELIHOOD OF
SUBSTRUCTURE IN CORONAL LOOPS

Kathryn McKeough¹
Vinay Kashyap² & Sean McKillop²

¹ Carnegie Mellon University, 5000 Forbes Ave, Pittsburgh, PA 15289, USA
² Harvard-Smithsonian Center for Astrophysics, 60 Garden St, Cambridge, MA 02138, USA

What can we see at very small spatial scales that help constrain the theories of coronal heating

Temperature range of Corona

Temperature of AIA

How far the sun is from earth

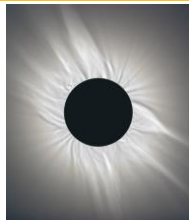
What wavelength AIA we are looking at (HiC is same)

Radius of the sun

Slide 2

Coronal Heating

- 500,000 - 3 million K
- 1000 times hotter than surface of sun
- Power required = ~ 1 kilowatt/ m²



<http://apod.nasa.gov/apod/ap090726.html>

Surface area of the sun 6.09×10^{12} km²

Corona, transition, chromosphere, photosphere....

where energy is coming from how it is being deposited (understandable because corona is lower density)

Slide 3

Coronal Loops

- Magnetic flux tube filled with hot plasma
- Connects regions of opposite polarity
- Potential location of coronal heating mechanisms



AIA 193 A 2012/07/11 18:53:44 (top)
<http://www.davidarling.info> (bottom)

Slide 4

Coronal Heating -Solutions

Nanoflares	Alfven Waves
<ul style="list-style-type: none">Small scaleSmall consecutive bursts of energy that contributes to heatingMagnetic reconnection induced by stresses from footpoint motions causing braids in flux tubes	<ul style="list-style-type: none">Large scaleAlfven waves dissipate energy into plasma through turbulenceWaves propagate along flux tubes

two types small scale v. large scale
Nanoflares – small compared to across the loop
Alfven Waves- long compared to the length of the loop
-propagate from center, but can be reflected back
- Not all energy caused by turbulence
- AW 0.08 m
footpoint= where loop enters chromosphere

Slide 5

Goal

By identifying the substructure of coronal loops, we determine dominant spatial scales and constrain theories of coronal heating.

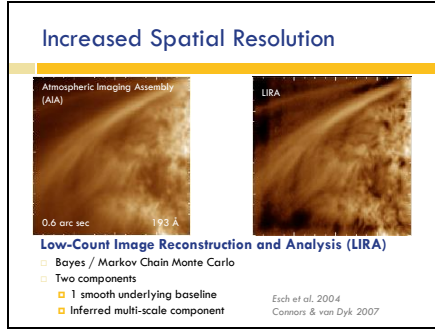
Slide 6

Increased Spatial Resolution

The slide shows a comparison of coronal loop images. The top row shows two images: 'Atmospheric Imaging Assembly (AIA)' on the left and 'High-resolution Coronal Imager (Hi-C)' on the right. Both images show a coronal loop with a red box highlighting a specific region. The bottom row shows two zoomed-in views of the region highlighted in the top row, with two parallel black lines indicating the spatial scale of the features. The timestamp '18:53:44' is visible in the bottom left of both images.

Model smooth variations of image
Bayesian multiscale method that uses MCMC
AIA on SDO since 2010

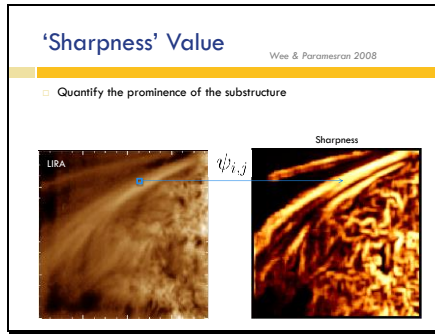
Slide 7



Model smooth variations of image
Arc second resolution of each
AIA is 1.3 arc min (77 arc sec) across
Bayesian multiscale method that uses
MCMC

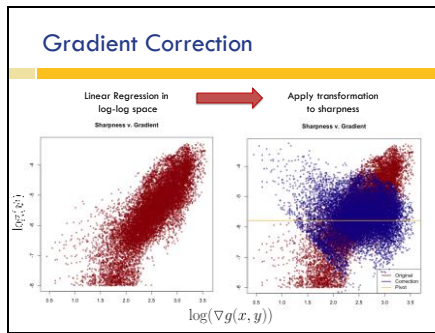
----- Meeting Notes (8/13/14 12:06) -----
Forward modeling process (start with
source, push through instrument to
compare to data)

Slide 8



----- Meeting Notes (8/13/14 12:06) -----
retitle LIRA on... --> sharpness
qualitatively explain sharpness value

Slide 9



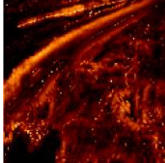
Detecting too many edges
Pivot data about horizontal using
function of gradient & linear regression
fit of sharpness v gradient in log-log
space

Slide 10

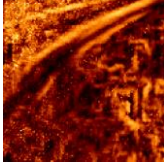
Significance of Substructure

- Null hypothesis = no substructure in coronal loop
- Null image = convolve observed image with PSF

LIRA on Observed Corrected Sharpness



LIRA on Null Image Corrected Sharpness



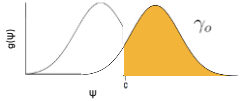
Slide 11

p-Value Upper Bound

Stein et al., 2014 (draft)

- 5 Poisson realizations of double convolved image
- Compare sharpness for the observed image (ψ_o) and the simulated images (ψ_n)

p-value upper bound $\hat{u} = \frac{\hat{\gamma}_n}{\gamma_o}$



QUESTION

Adjacent sharpness are correlated

P-value test is independent?

Draw gamma_o curve

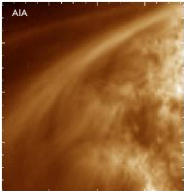
what we chose for gamma_n (=0.05)

Slide 12

p-Value Upper Bound

- Significant sharpness: $\hat{u} < 0.06$

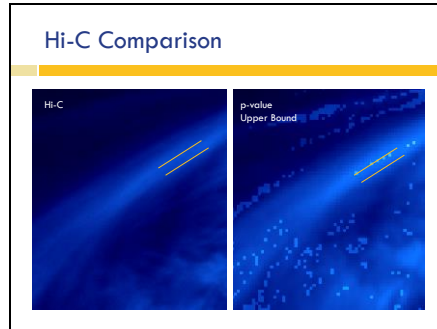
AIA



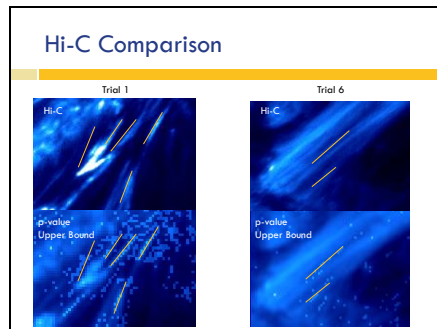
p-value Upper Bound



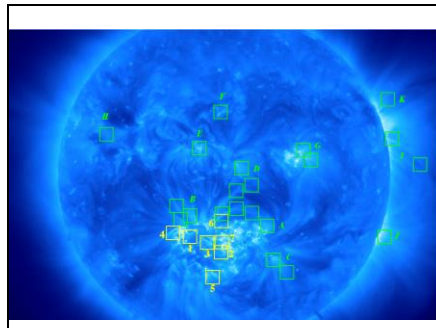
Slide 13



Slide 14



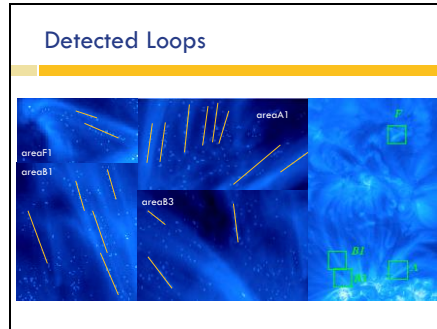
Slide 15



For each of the loops, we are able to see if there is substructure
If all loops come up with substructure – strands everywhere (low lying, upper corona etc.)

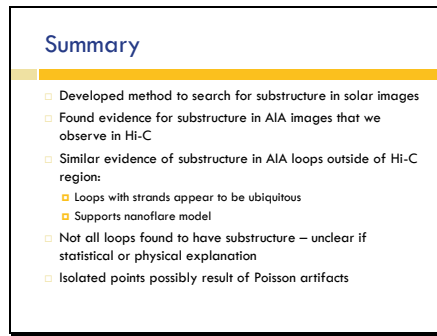
Apply to different regions of the sun to determine where along the loops substructure exists and therefore where we expect to see these coronal heating phenomena.

Slide 16

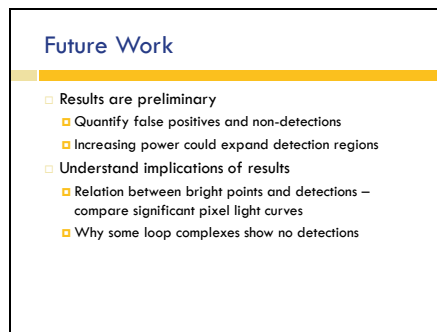


Those that don't may have not been detected
those that do have strong indication of substructures
More likely to be heated by nanoflares in future

Slide 17



Slide 18



quantify= poisson artifacts
Power = simulations

Slide 19

Acknowledgements

We acknowledge support from AIA under contract SPQ2H1701F from Lockheed-Martin to SAO.

We acknowledge the High resolution Coronal Imager instrument team for making the flight data publicly available. NASA/NASA and the mission and partners include the Smithsonian Astrophysical Observatory in Cambridge, Mass.; Lockheed Martin's Solar Astrophysical Laboratory in Palo Alto, Calif.; the University of Central Lancashire in Lancaster, England; and the Lebedev Physical Institute of the Russian Academy of Sciences in Moscow.

Vinay Kalyap acknowledges support from NASA Contract to Chandra X-ray Center NAS8-03060 and Smithsonian Competitive Grants Fund 40488100HH0043.

We thank David van Dyk and Nathan Stein for useful comments and help with understanding the output of URA.



Slide 20

Bibliography

Brooks, D. et al. 2013, *Apl*, 722L, 198
Cargill, P., & Klimchuk, J. 2004, *Apl*, 605, 911C
Connors, A., & van Dyk, D. A. 2007, *Statistical Challenges in Modern Astronomy IV*, 371, 101
Cramer, S., et al. 2012, *Apl*, 754, 92C
Cramer, S., et al. 2007, *AplS*, 171, 520C
DeForest, C. E. 2007, *Apl*, 661, 532D
Bali, D. N., Connors, A., Katsouris, M., & van Dyk, D. A. 2004, *Apl*, 610, 1213
Narasimhan, S., & Klimchuk, J. 2005, *Apl*, 628, 1023P
Raymond, J. C., et al. 2014, *Apl*, 788, 152R
Viall, N. M., & Klimchuk, J. 2011, *Apl*, 738, 24V
Wu, C. Y., & Foramenron, R. 2008, *ICSP2008 Proceedings*, 978-1-4244-2179-4/08

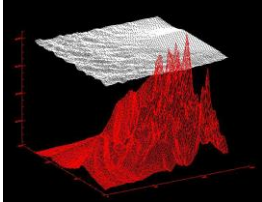
Slide 21

Extra Slides

Slide 22

Baseline Model

1. Begin with max
2. Correct using min curvature surface through convex hull
3. Iterate until surface lies below data



The image shows a 3D plot with a red surface and a grey plane. The red surface is being adjusted to fit a set of data points (represented by small red dots) that are scattered below the grey plane. The surface is being corrected using a min curvature method through a convex hull.

Correction never more than 5%
----- Meeting Notes (8/13/14 12:06) -----
BYE BYE SLIDE

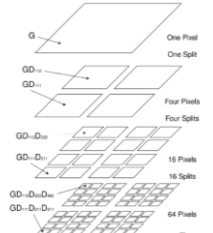
Slide 23

LIRA Operations

INPUT	OUTPUT
<ul style="list-style-type: none">□ Point Spread Function (PSF)□ Observed Image ($2^n \times 2^n$)□ Baseline Model□ Prior & Starting Image	<ul style="list-style-type: none">□ MCMC iterations of Multi-scale Counts□ Posterior distribution of departures from baseline□ De-convolution

Slide 24

Multi-scale Representation



The diagram illustrates a multi-scale representation of a grid. It shows a sequence of grids with increasing resolution. The top grid is labeled 'One Pixel One Split'. The next grid is labeled 'Four Pixels Four Splits'. The third grid is labeled '16 Pixels 16 Splits'. The fourth grid is labeled '64 Pixels'. The labels for the grids are: G , GD_{-1} , GD_{-2} , GD_{-3} , GD_{-4} , GD_{-5} , GD_{-6} , GD_{-7} , GD_{-8} .

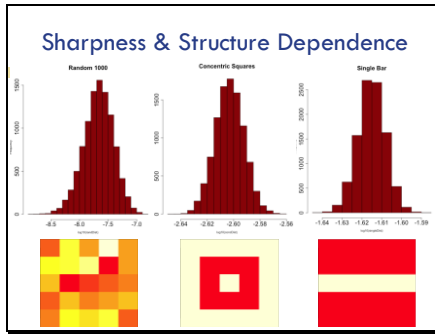
Slide 25

'Sharpness' Value

$g(x,y)$	→	Image matrix
$\tilde{g}(x,y) = \frac{g(x,y)}{\sqrt{\sum_{x=0}^{N-1} \sum_{y=0}^{N-1} [g(x,y)]^2}}$	→	Normalization
$G = \tilde{g}(x,y) - \mu$	→	Subtract mean
$S_{\tilde{g}} = \frac{1}{(N-1)} GG^T$	→	Covariance matrix
$S_{\tilde{g}} = UDV$	→	Singular Value Decomposition
$\sum_{i=1}^N \lambda_i^2 = \psi^2$	→	Sum of squared eigenvalues (diagonal of D)

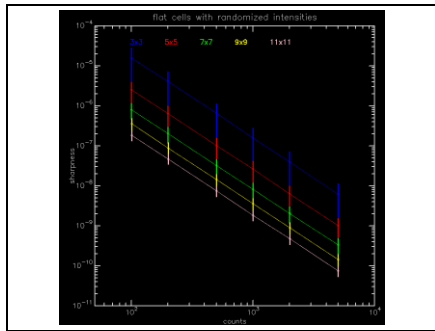
----- Meeting Notes (8/13/14 12:06) -----
EXTRA SLIDE

Slide 26



Random, X and randomized

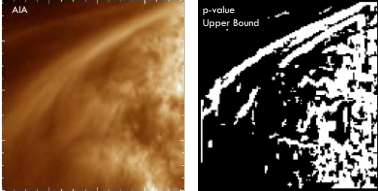
Slide 27



Slide 28

Edge Detection

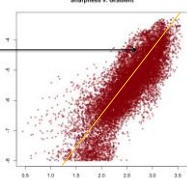
- Gradient steepest along edges → edge detection



The slide shows two images side-by-side. The left image is a brown-toned astronomical image labeled 'AIA'. The right image is a black and white edge detection image of the same scene, labeled 'p-value Upper Bound'.

Slide 29

Gradient Correction

$$\psi' = 10^{\log(\psi) - (a \times \log(\nabla g) - \bar{\nabla} g)}$$
$$\log(\psi) = a \times \log(\nabla g) + b$$


The slide features a scatter plot titled 'Sharpness x Gradient'. The x-axis ranges from 0.0 to 3.0, and the y-axis ranges from 0.0 to 1.0. The plot shows a dense cloud of red data points with a red regression line indicating a positive correlation. A horizontal line from the equation $\log(\psi) = a \times \log(\nabla g) + b$ points to the regression line.